Extremely Stable Luminescent Crosslinked Perovskite Nanoparticles under Harsh Environments over 1.5 Years

Junho Jang, Young-Hoon Kim, Sunjoong Park, Dongsuk Yoo, Hyunjin Cho, Jinhyeong Jang, Han Beom Jeong, Hyunhwan Lee, Jong Min Yuk, Chan Beum Park, Duk Young Jeon, Yong-Hyun Kim, Byeong-Soo Bae,* and Tae-Woo Lee*

Organic–inorganic hybrid perovskite nanoparticles (NPs) are a very strong candidate emitter that can meet the high luminescence efficiency and high color standard of Rec.2020. However, the instability of perovskite NPs is the most critical unsolved problem that limits their practical application. Here, an extremely stable crosslinked perovskite NP (CPN) is reported that maintains high photoluminescence quantum yield for 1.5 years (>600 d) in air and in harsher liquid environments (e.g., in water, acid, or base solutions, and in various polar solvents), and for more than 100 d under 85 °C and 85% relative humidity without additional encapsulation. Unsaturated hydrocarbons in both the acid and base ligands of NPs are chemically crosslinked with a methacrylate-functionalized matrix, which prevents decomposition of the perovskite crystals. Counterintuitively, water vapor permeating through the crosslinked matrix chemically passivates surface defects in the NPs and reduces nonradiative recombination. Green-emitting and white-emitting flexible large-area displays are demonstrated, which are stable for >400 d in air and in water. The high stability of the CPN in water enables biocompatible cell proliferation which is usually impossible when toxic Pb elements are present. The stable materials design strategies provide a breakthrough toward commercialization of perovskite NPs in displays and bio-related applications.

Organic–inorganic hybrid perovskites (OIHPs), with ABX_3 structure (A: organic cation, B: metal cation, X: Cl^-, Br^-, I^-), have emerged as a new class of material for opto-electronics.[1–3] The power conversion efficiency of OIHPs in photovoltaic cells has been increased to >25.2%.[4] OIHPs also show promise as light emitters in display and bioimaging applications because of low material cost, facile wavelength tunability, high photoluminescence (PL) quantum yield (QY), and narrow spectral emission (full width at half-maximum (FWHM) of <25 nm), which allow them to achieve wide color gamut (≈140% of National Television Systems Committee (NTSC) 1931 and >95% of International Telecommunication Union Recommendation BT.2020 standard (Rec.2020)).[5,6] A significant breakthrough in electroluminescence efficiency has been achieved in self-emissive light-emitting diodes (LEDs) that use OIHP films as light-emitting layers. External quantum efficiency (EQE) has been increased to 21.6% in LEDs that use OIHP polycrystalline bulk

Dr. J. Jang, H. Lee, Prof. B.-S. Bae
Wearable Platform Materials Technology Center
Korea Advanced Institute of Science and Technology (KAIST)
291 Daehak-ro, Yuseong-gu, Daejeon 34141, Republic of Korea
E-mail: bsbae@kaist.ac.kr

Dr. J. Jang, Dr. S. Park, H. Cho, J. Jang, H. B. Jeong, H. Lee,
Prof. J. M. Yuk, Prof. C. B. Park, Prof. D. Y. Jeon, Prof. B.-S. Bae
Department of Materials Science and Engineering
Korea Advanced Institute of Science and Technology (KAIST)
291 Daehak-ro, Yuseong-gu, Daejeon 34141, Republic of Korea

Dr. Y.-H. Kim, Prof. T.-W. Lee
Department of Materials Science and Engineering
Institute of Engineering Research
Research Institute of Advanced Materials
Nano Systems Institute (NSI)
BK21 PLUS SNU Materials Division for Educating Creative Global Leaders
Seoul National University
1 Gwanak-ro, Gwanak-gu, Seoul 08826, Republic of Korea
E-mail: twlees@snu.ac.kr

Dr. D. Yoo, Prof. Y.-H. Kim
Department of Physics
Korea Advanced Institute of Science and Technology (KAIST)
291 Daehak-ro, Yuseong-gu, Daejeon 34141, Republic of Korea

Prof. Y.-H. Kim
Graduate School of Nanoscience and Technology
Korea Advanced Institute of Science and Technology (KAIST)
291 Daehak-ro, Yuseong-gu, Daejeon 34141, Republic of Korea

Prof. T.-W. Lee
School of Chemical and Biological Engineering
Seoul National University (SNU)
1 Gwanak-ro, Gwanak-gu, Seoul 08826, Republic of Korea

**ADVANCED
SCIENCE NEWS**
www.advancedsciencenews.com

**ADVANCED
MATERIALS**
www.advmat.de

films,[7] and to 21.3% in LEDs that use colloidal OIHP nanoparticles (NPs).[8] Color-converting LEDs (CC-LEDs) that use OIHPs as a color-converting layer which is placed in front of a backlight unit have achieved higher PLQY (>70%) and wider color gamut (FWHM <25 nm, 130% of NTSC)[9] than those of CC-LEDs that use Cd-based inorganic quantum dots (QDs) (PLQY: 60%, FWHM: 30 nm, ≈110% of NTSC)[10,11] and In-based inorganic QDs (PLQY: ≈70%, FWHM: 40 nm, ≈90% of NTSC).[12,13] However, OIHPs are chemically unstable; this demerit limits their practical application in displays and lighting.
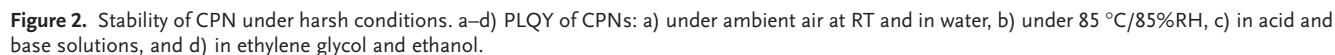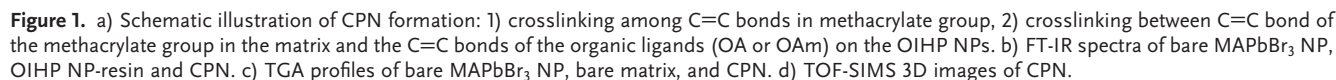
OIHP polycrystalline films in humid or high temperature environments are vulnerable to decomposition of perovskite crystals,[3,14] to ion migration,[15] and to development of metastable states.[16] Stability of OIHPs can be improved in the form of colloidal NPs in which surface-covering organic ligands prevent ion migration and permeation of water and oxygen.[17,18] Stability of OIHP NPs has been further increased by various methods such as formation of an inorganic shell (e.g., Al_2O_3 or SiO_2),[19] Janus structures,[20] heterojunction structures[21] and NP/polymer composites.[22,23] However, such strategies still showed limited stability of OIHP NPs under ambient air or in water, and entail complex processes to prevent aggregation of NPs in polymer matrixes.[22,23] Moreover, OIHP NPs that are stable under harsh conditions (acid or base solutions, polar solvents, high temperature with high humidity) have not been reported. Especially, methylammonium ($CH_3NH_3^+$, MA) based OIHPs decay faster in the presence of moisture than do others such as formamidinium or mixed-cation based OIHPs.[3,24] Therefore, highly stable and uniformly dispersed OIHP NP composites without complex processes such as ligand-exchange and formation of an inorganic shell are desirable.

Herein, we report a simple but effective materials-design approach to achieve extraordinarily-long stability of crosslinked MA lead bromide ($MAPbBr_3$) NPs in various environments (air, water, chemicals, high temperature (85 °C) with high relative humidity (85%RH) (85 °C/85%RH)) by employing methacrylate-functionalized matrix. The methacrylate in the matrix induces a crosslinking with unsaturated hydrocarbon in acid and base ligands (oleic acid, OA; oleylamine, OAm) in OIHP NPs at a molecular scale, to form a crosslinked perovskite NP (CPN) that prevents decomposition of MA from the perovskites and achieves homogeneous distribution of NP in the matrix. Moreover, the low concentration of moisture that diffuses through the crosslinked matrix during aging can chemically heal surface defects in the NPs, and thereby reduce nonradiative recombination in CPN. As a result, CPNs showed high PLQY of ≈70% which remained for >600 d in air, water and acid or base solutions, and various polar solvents, and for >100 d under 85 °C/85%RH. Resulting CPN-based CC-LEDs showed wide color gamut ($MAPbBr_3$-based CPN: 120% of NTSC 1931 and 89% of Rec. 2020; $CsPbBr_3$-based CPN: 130% of NTSC 1931 and 97% of Rec.2020) and demonstrated natural white-emission with color-tunability and excellent stability (high PLQY for >400 d at RT in ambient air and in water) by integration with red-emissive Cd base QDs. Flexible large-area CC-LEDs based on CPN were also demonstrated. Moreover, water- and chemical-persistent CPNs were successfully applied to cell proliferation which has been impossible with water-sensitive materials with toxic elements (e.g., Cd and Pb).[25]

CPNs were synthesized by UV-induced free-radical reaction of OIHP NP-dispersed methacrylate-functionalized matrix resin (OIHP NP-resin) (**Figure 1**a). The $MAPbBr_3$ NPs (0.5 wt% of obtained resin, average size ≈ 9.06 nm, standard deviation ≈1.59 nm) (Figures S1a, S2a, and Table S1, Supporting Information) were uniformly mixed with precursors of resin ((3-methacryloxypropyl)trimethoxysilane (MPTS), diphenyl-silanediol (DPSD)) by hydrophobic interaction between functional groups (methacrylate and phenyl groups) in precursors and unsaturated organic ligands (OA binds as oleate, and OAm binds as oleylammonium) in NPs.[26,27] Then, viscous OIHP NP-resin was obtained by chemical reaction between methoxy group ($Si-OCH_3$) of MPTS and hydroxyl group ($Si-OH$) of DPSD at elevated temperature (80 °C) (Inset in Figure S3, Supporting Information). Finally, CPN was solidified by UV-curing, which induces two different free-radical cross-linking reactions: 1) between two C=C bonds in methacrylate groups in matrix; and 2) between C=C bond in methacrylate group and C=C bond in surface organic ligands (OA and OAm) of OIHP NPs.[11] Solidified CPNs showed highly condensed (87% of degree of Si-O-Si bond formation from silane precursors, Figure S3 and Table S2, Supporting Information) and amorphous SiO_2-like matrix (ladder-like Si-O-Si structure, Figure S4, Supporting Information).[28] The solidified CPNs showed similar NP size but slightly redshifted PL spectrum to those of colloidal OIHP NP solution most probably due to generated defects during UV-curing (will be discussed below) (Figure S5, Tables S1 and S3, Supporting Information).

Chemical linkage between methacrylate-functionalized matrix and OIHP NPs was confirmed by Fourier-transform infrared (FT-IR) and thermogravimetric analysis (TGA) (Figure 1b,c). Cross-linking reaction between surface ligands of OIHP NPs and methacrylate groups of matrix was confirmed by almost disappearance of the C=C bond peak at 1000–950 cm^{-1} in FT-IR, and by increased decomposition temperature (T_d at 5% weight loss = 382 °C) of CPN compared to those of bare matrix (355 °C) and pristine OIHP NPs (185 °C) in TGA.[11] On the contrary, CPN based on OIHP NPs with other ligands that do not have unsaturated carbon double bonds showed decreased T_d (253–353 °C) compared to those of the bare matrix (Figure S6, Supporting Information); this difference confirms the important function of crosslinking between methacrylate in matrix and unsaturated hydrocarbon in both acid and amine ligands (OA and OAm) in OIHP NPs. Uniform distribution of OIHP NPs in CPNs was confirmed by time-of-flight secondary-ion mass spectroscopy (TOF-SIMS) (Figure 1d) and dispersive-Raman PL spectroscopy (Figure S7, Supporting Information). The resulting PLQY of CPNs was relatively low (≈15%) due to photoactivated defects that generated during UV-induced free-radical reaction.[29] The presence of defects was confirmed by decreased PL lifetime (Figure S8, Supporting Information) and redshifted PL spectrum in as-cured CPN compared to those of OIHP NP solution and before UV-cured resin (Figure S5 and Table S3, Supporting Information).

To investigate the stability of the CPNs, we measured their PLQY under various aging conditions. Surprisingly, the CPNs showed gradually increasing PLQY, from ≈15% to ≈70% during first 2 d; then maintained it for >1.5 years (600 d) under ambient air at room temperature (RT) and even in water (**Figure 2**a). These increased PLQY values were similar to those of colloidal

Figure 1. a) Schematic illustration of CPN formation: 1) crosslinking among C=C bonds in methacrylate group, 2) crosslinking between C=C bond of the methacrylate group in the matrix and the C=C bonds of the organic ligands (OA or OAm) on the OIHP NPs. b) FT-IR spectra of bare MAPbBr$_3$ NP, OIHP NP-resin and CPN. c) TGA profiles of bare MAPbBr$_3$ NP, bare matrix, and CPN. d) TOF-SIMS 3D images of CPN.

Figure 2. Stability of CPN under harsh conditions. a–d) PLQY of CPNs: a) under ambient air at RT and in water, b) under 85 °C/85%RH, c) in acid and base solutions, and d) in ethylene glycol and ethanol.

OIHP NP films coated on glass (PLQY: 73%); this observation indicates that the optical property in CPNs had been recovered by aging (Table S4, Supporting Information). CPNs that is aged under 85 °C/85%RH also showed increased PLQY to ≈60% which was then retained for 100 d (Figure 2b). As PLQY increased, the PL spectrum of CPNs blueshifted although aged CPNs showed similar average NP size to the as-cured CPN (before aging) (Table S1, Supporting Information); this trend implies defect passivation under aging (Figure S9, Supporting Information). CPNs based on OIHP NPs with different ligands that do not have unsaturated carbon double bonds showed decreasing PLQY under 85 °C/85%RH (Figure S10, Supporting Information). Furthermore, composites with other green light emitters such as an organic emitter (tris(8-hydroxyquinolinato) aluminum, Alq$_3$), an InP/ZnS QD (ligand: 1-dodecanthiol), and a CdSe/CdZnS QD (ligands: OA and trioctylphosphine), showed decrease in PLQY (Alq$_3$: from 20% to 5%; InP/ZnS QD: from 50% to 30%; CdSe/CdZnS QD: from 46% to 10% after 80 d) (Figure S11, Supporting Information) due to the absence of crosslinking between methacrylate groups in matrix and ligands of emitters. Moreover, colloidal MAPbBr$_3$ NP solution showed rapid decrease in PLQY down to ≈0% within few second in water and under 85 °C/85%RH. These results confirm that chemical crosslinking between methacrylate group in matrix and unsaturated carbon double bonds of both acid and amine ligands of light-emitters is an important prerequisite for photophysical recovery and increased stability under aging.

The CPNs also exhibited increased PLQY of ≈70%, which was then retained for >600 d in acid (0.1 M HCl) and base (0.1 M NaOH) solutions as well as in various polar solvents (ethylene glycol and ethanol, which cause decomposition and degradation of perovskite crystals);[30] these results indicate that the CPNs had the excellent chemical stability (Figure 2c,d). CPNs showed increased PLQY (≈50%) and maintained it under continuous blue-light irradiation (wavelength λ = 460 nm) in ambient air (Figure S12, Supporting Information); this result demonstrates the excellent photostability of the CPNs. The CPNs showed consistent NP size (before aging: average size ≈ 10.5 nm, standard deviation ≈1.82 nm; after aging: average size ≈ 10.56 nm, standard deviation ≈ 1.63 nm) without any distinct aggregation after aging (Figures S1b–d, S2b–d, and Table S1, Supporting Information); this result indicates that the increased PLQY is due to chemical interaction rather than changes of physical morphology or aggregations of OIHP NPs.

To investigate the recombination dynamics of CPNs, we measured PL lifetimes by conducting time-correlated single-photon counting analysis (**Figure 3**a). The PL decay curves were fitted using a biexponential decay model, which reveals a fast-decay component (time, τ_1; fraction, f_1) and a slow-decay component (τ_2, f_2). Fast decay is related to trap-assisted nonradiative recombination, whereas slow decay is related to radiative recombination.[5,17,31] First, all CPN samples and OIHP NP-resin (before UV-curing) showed much longer PL lifetime than colloidal OIHP NPs possibly due to the interaction with resin precursors (Figure S13, and Table S5, Supporting Information).[32,33] Due to defect passivation, τ_2, f_2, and calculated average PL lifetime increased under aging (Table S5, Supporting Information); this result corresponds well to the increased PLQY and blueshifted PL spectrum. We calculated

the radiative and nonradiative recombination rates of each CPN by using obtained PL lifetime and PLQY as

$$\frac{1}{K} = \frac{1}{K_{nr} + K_r} \tag{1}$$

$$\text{PLQY} = \frac{K_r}{K_{nr} + K_r} \tag{2}$$

where K_r is radiative rate, K_{nr} is nonradiative rate and K is PL decay rate (= reciprocal of PL lifetime) (**Table 1**). As-cured CPNs (before aging) had K_r ≈ 0.003 ns^{-1} and K_{nr} ≈ 0.017 ns^{-1}. Aged CPNs showed increased K_r ≈ 0.009 ns^{-1} and reduced K_{nr} ≈ 0.004 ns^{-1}, which are similar to those of OIHP NP-resin (before UV-curing); this result indicates that aging can maximize the number of radiative pathways while minimizing the number of nonradiative pathways.

To study the defect passivation mechanism, we conducted FT-IR measurements of CPNs before and after aging (Figure S14, Supporting Information). The peaks attributed to the Si—O—Si bond (1000–1100 cm^{-1}), to the C=O bond in methacrylate and OA (1700–1720 cm^{-1}) and to the COO$^-$ bond in methacrylate and OA (1540–1570 cm^{-1}) did not change, but a peak attributed to the hydroxyl group (-OH) (3700–3150 cm^{-1}) occurred after aging. These results indicate that water molecules, which can induce defect passivation on OIHP NPs, are absorbed in the CPN during aging without changing other chemical bonds. Methacrylate-functionalized matrix has a water-vapor transmission rate of 4 g m^{-2} day^{-1}, which confirms that water molecules can penetrate the CPNs and interact with OIHP NPs (Figure S15, Supporting Information). CPNs did not show any PLQY increase under aging in vacuum, nitrogen, and oxygen environments (Figure S16, Supporting Information); these results support our hypothesis that water molecules passivate defects, in accordance with previous literature.[34]

To obtain insight into the defect passivation in CPNs by water molecule, we performed X-ray photoelectron spectroscopy (XPS) analysis (Figure 3b and Figure S17, Supporting Information). As-cured CPNs showed XPS peaks regarding unsaturated Pb (≈137 eV and ≈142 eV) (black in Figure 3b)[5,17] which can be assigned to the metallic Pb (Pb(0)) due to the metallic characteristics, that acts as an exciton quencher and reduces PLQY.[5,17] After aging, CPNs did not show metallic Pb peaks (green: RT in ambient air, blue: in water, red: 85 °C/85%RH in Figure 3b); this disappearance indicates that water molecules can passivate Br-vacancy defects (i.e., remove metallic Pb).[5,17] Also, the N peak of CPN did not change after aging, therefore we conclude that MA from perovskites is not decomposed by water (Figure S18, Supporting Information).[29]

To understand how Br-vacancy defects in CPNs are passivated by water molecules at a microscopic level, we conducted first-principles density-functional theory (DFT) calculations on the adsorption of water molecules on both (100) and (110) surfaces. We considered the OIHP NPs surfaces to be Br-deficient because the OIHP NPs in CPN have an off-stoichiometric Pb/Br composition (Table S6, Supporting Information), which can form surface halide vacancies (i.e., metallic Pb) and electronic trap states.[30,35]
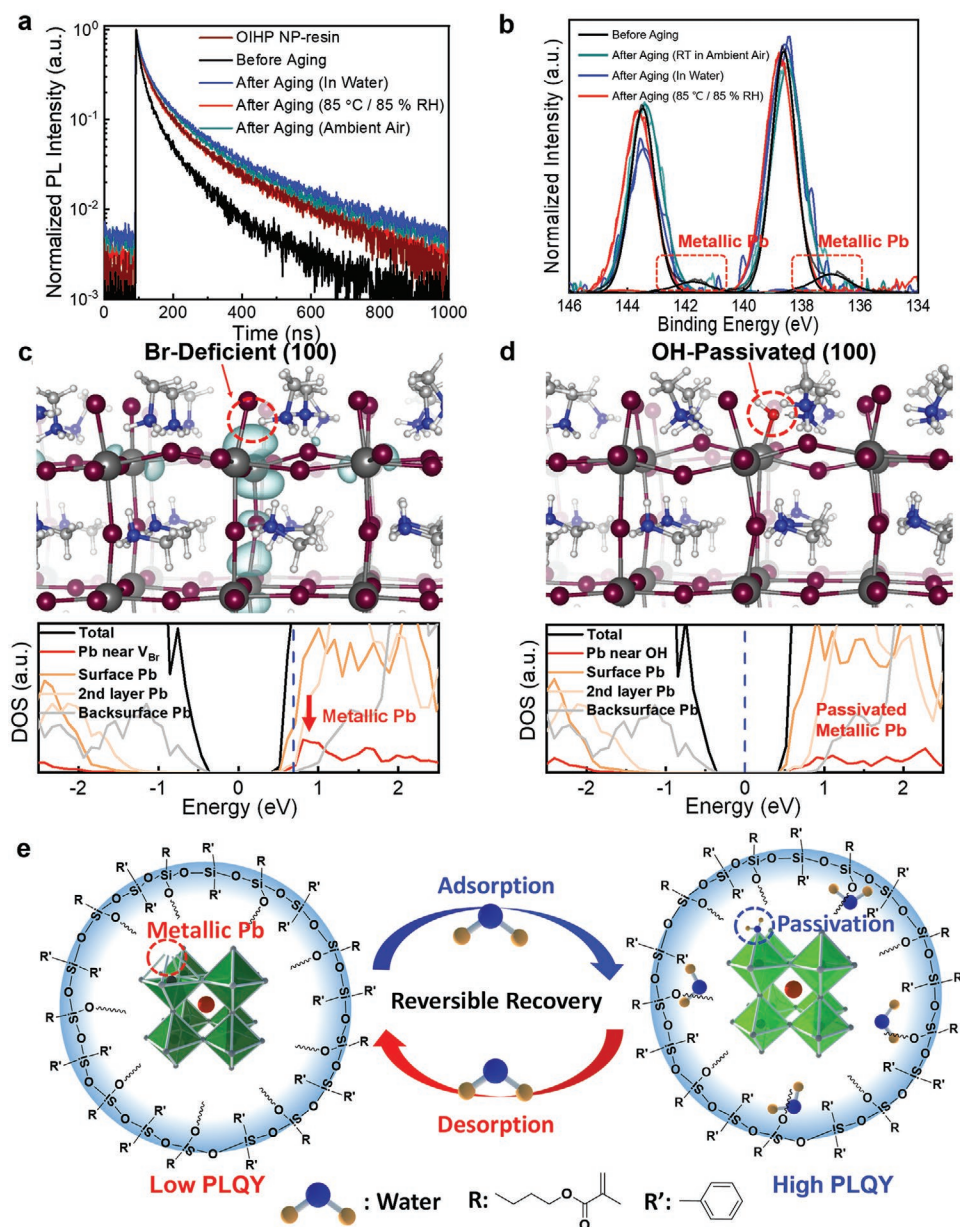
ADVANCED
SCIENCE NEWS
www.advancedsciencenews.com

ADVANCED
MATERIALS
www.advmat.de

Figure 3. a) PL decay dynamics of OIHP NP-resin, CPN before and after aging at RT in ambient air, water and 85 °C/85%RH. b) XPS spectra (Pb 4f peaks) of CPN before and after aging under RT in ambient air, water, and 85 °C/85%RH. c,d) Side views of ball-and-stick models of Br-deficient (c) and OH-passivated (d) (100) MAPbBr$_3$ surfaces (wine: Br, blue: N, gray: Pb, red: O) and their density of states profiles near the Fermi energy level (broken blue line). Red arrow: metallic Pb state. e) Schematic illustration of reversible defect healing in CPN by H$_2$O molecules.

Table 1. Summary of PLQY, PL lifetime, K_r and K_{nr} of colloidal OIHP NPs, OIHP NP-resin, CPN before and after aging.

Conditions	PLQY [%]	Lifetime [ns]	K_r [ns^{-1}]	K_{nr} [ns^{-1}]
Colloidal OIHP NPs	73	31.7	0.0230	0.0089
before UV-curing (OIHP NP-Resin)	70	66.5	0.0105	0.0045
Before aging	15	49.3	0.0030	0.0172
RT in ambient	70	81.3	0.0086	0.0036
85 °C/85%RH	70	74.7	0.0093	0.0040
In water	70	81.8	0.0085	0.0037

Calculation results showed that a surface Br vacancy on the (100) (3 × 3) surface produces a metallic character (under-coordinated Pb) with localized (deep) defect states above the conduction band minimum (Figure 3c). By introducing an –OH group, we obtained perfect passivation of defective (100) surfaces, and electronic stabilization (Figure 3d). Also, the anionic OH bonded directly to the (110) (2 × 2) surface in locations where full coverage of Br had failed, and thereby electronically passivated the metallic Pb sites on the (110) surface (Figure S19a–c, Supporting Information). Although the bare (110) surface can be fully passivated by both Br and OH groups, water molecules can also bind to both Br-passivated

**ADVANCED
SCIENCE NEWS**
www.advancedsciencenews.com

**ADVANCED
MATERIALS**
www.advmat.de

and OH-passivated (110) surfaces, and thereby make the electronic structures intact (Figure S19d, Supporting Information). The binding energies of the –OH group (0.19–1.49 eV/molecule) and H_2O molecule (0.82 eV/molecule) on the OIHP surfaces are much lower than that of Br (1.78–2.54 eV/molecule); that is, the –OH group and H_2O molecule are weakly bonded and can be easily detached (Table S7, Supporting Information). Following the DFT calculations for the weakly bonded –OH group on the surface, we observed reversible PLQY change under repetitive aging by adsorption of water molecules (Figure S20, Supporting Information). Furthermore, to investigate the effects of precursor ratio on the stability of CPN, we synthesized CPN based on NPs with excess Br (molar ratio of $MABr:PbBr_2 = 1.5:1$ or 2:1) (Figure S21, Supporting Information). CPN based on NPs with excess Br showed PLQY (47% of 1.5:1, 56% of 2:1) which is higher than that based on NPs with equimolar precursor ratio (PLQY ≈ 15%) because excess Br suppresses the defect formation during UV-curing. However, the CPN based on NPs with excess Br exhibited gradually decreasing PLQY under aging in ambient air at RT, water and 85 °C/85%RH conditions with a function of time, which indicates that defect passivation effect of water molecules is inefficient. Therefore, we can claim that equivalent molar ratio between precursors is necessary to achieve the high stability of CPN although it shows relatively low initial PLQY in as-cured CPN. Therefore, our calculations and experiments are consistent with hypothesis that OIHP NPs are chemically bonded to the methacrylate-functionalized matrix, and induce reversible healing of the defect states by water molecules (Figure 3e).

To demonstrate the feasibility of using CPNs as a color-converting layer in CC-LEDs, we fabricated green-emitting CC-LEDs that used CPNs (**Figure 4**a), and white-emitting CC-LEDs integrated with red-emitting composite that use CdSe/CdZnS QDs (Figure 4b). CC-LEDs successfully achieved blue-to-green conversion of light emitted from a mobile phone screen (left in Figure 4c) and blue-to-white conversion of light emitted from a blue LED chip (left in Figure 4d). We also demonstrate the operation of flexible large-area (size: 10 cm × 10 cm) color-converting films under bending (right in Figure 4c,d). The fabricated CC-LEDs covered the 120% of NTSC 1931 and 89% of Rec. 2020; these coverages are wider than those of green Cd-based QD due to its narrower FWHM (22 nm) and shorter emission peak (530 nm) (Figure 4e and Figure S22, Supporting Information). White-emitting CC-LEDs also showed increasing PLQY from 28% to 60% which retained for >400 d under aging at RT in ambient air and in water (Figure 4f). Under aging, white-emitting CC-LEDs showed a gradual change of Commission Internationale de l'Eclairage coordinates from (0.300, 0.166) (reddish white) to (0.316, 0.318) (natural white) (Figure S23, Supporting Information) and increased green emission peak (Figure 4g, Figures S24 and S25, Supporting Information); these changes indicate the color-tunability of our CC-LEDs. These results indicate that as a color converting layer in CC-LEDs, the CPNs have advantages of higher PLQY, narrower spectral linewidth, lower material cost, higher stability against water, high temperature with high humidity and chemicals over other green-emitting composites that use Cd- or In-based QDs (Table S8, Supporting Information).

To extend our crosslinked perovskite NP design strategy, we synthesized a $CsPbBr_3$ NP (ligands: OA and OAm)-based CPN.

$CsPbBr_3$ NP-based CPN had excellent stability with increasing PLQY in water (Figure S26, Supporting Information) and wide color gamut (130% of NTSC 1931 and 97% of Rec.2020) because $CsPbBr_3$-NP-based CPN has very narrow FWHM (19 nm) and short emission spectra (520 nm) (Figure 4e and Figure S22, Supporting Information). This result demonstrates the wide usability of our CPN materials using various perovskite crystals.

Water- and chemical-persistent CPN is a highly biocompatible material having outstanding stability of photoluminescence. To test this, we proliferated C2C12 mouse skeletal myoblast cells on the pristine OIHP NPs, CPNs, and sterilized-polystyrene cell culture plate (control experiment) using Cell Counting Kit-8 (CCK-8) assay (Figure 4h). For cell proliferation, we used water-based cell growth media containing Dulbecco's modified Eagle medium (DMEM) and fetal bovine serum (FBS). After culturing for 3 and 5 days, the number of living cells on the CPN films was increased significantly (i.e., increased optical density of the results of CCK-8 assay; O.D. from 0.7 to 3), which is even slightly higher than the control experiment (cell proliferation on sterilized-polystyrene cell culture plate) (from 0.7 to 2.8). Living cells on the pristine OIHP NPs cannot proliferate because water-based medium solution causes the direct decomposition of the lead halide perovskite crystals. Bright-field images directly showed the well-grown cells on the CPN films after culturing (Figure 4i); there results indicate that our CPN is biocompatible and has exceptional stability in water-based solutions during cell proliferation and its potential use can be extended to various biomedical optoelectronic applications on inside biological body that requires high stability under water and harsh environments.

These data provide three insights. 1) We determine that for crosslinked emitters to be stable, they must have chemical crosslinking between matrix and ligands of light emitting NPs; 2) We understand how the crosslinked matrix prevents the exposure of emitters to excess moisture and retains moderate concentration of water molecule surrounding the emitters; 3) We illustrate the competing effects of hydrolysis and defect passivation by water molecules surrounding perovskite crystals and show how to make defect passivation outcompete hydrolysis.

In conclusion, we have developed a materials-design strategy to increase the stability of perovskite NPs against ambient air, water, chemicals (polar solvents, acid, and base solutions) and heat. The method uses UV-induced free-radical crosslinking reaction between unsaturated hydrocarbon surface ligands of perovskite NPs and methacrylate-functionalized matrix to fabricate CPN with uniform dispersion of perovskite NPs. The crosslinked matrix suppresses hydrolysis of perovskite crystals by physically mitigating the exposure of perovskite crystals to excess moisture; the resulting moderate amount of water molecules chemically passivate surface defects in NPs when perovskite NPs have unsaturated carbon double bonds in both acid and base ligands. CPNs exhibited dramatically increased PLQY, from ≈15% to ≈70% after aging, then maintained such high PLQY for >600 d in ambient air at RT, in water, acid or base solutions, and various polar solvents and for >100 d in 85 °C/85%RH; this is the first report of such outstanding stability of perovskite NPs in various severe conditions. By conducting photophysical analysis and DFT calculations, we determine that the −OH group from water molecules
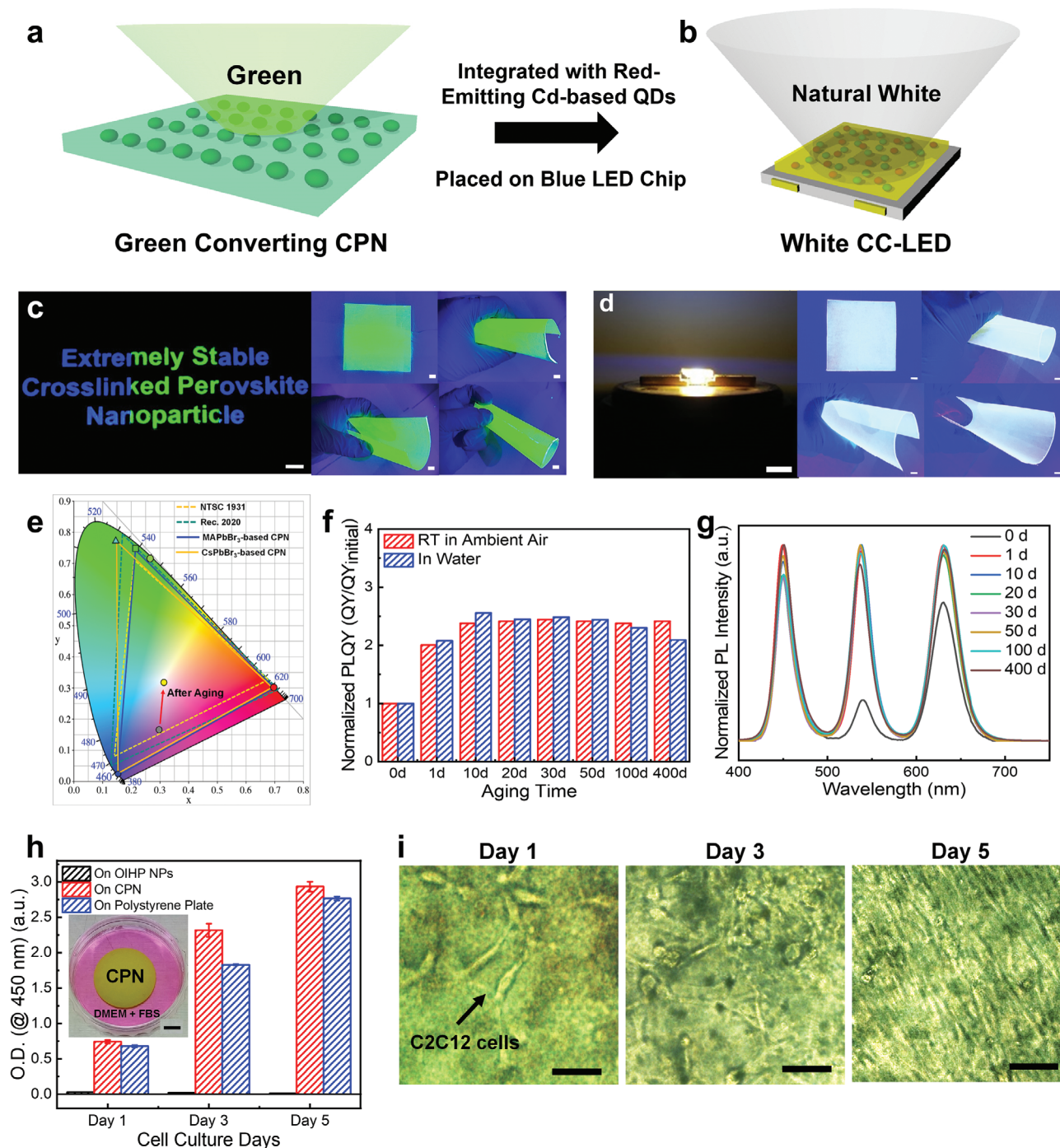
Figure 4. a,b) Schematic structures of a CPN-based green-emitting CC-LED (a) and a white-emitting CC-LED (b). c,d) Photographs of green CPN films on a blue-emitting mobile phone screen (left), flexible large-area (size: 10 cm × 10 cm) green-emitting CPN films under bending (right) (c), and a white CC-LED on a blue-LED chip (left) and flexible large-area (size: 10 cm × 10 cm) white-emitting CPN films under bending (right) (d). Scale bars in photographs are 1 cm. e) Emission plots of CC-LEDs based on crosslinked MAPbBr$_3$ NP and crosslinked CsPbBr$_3$ NP, NTSC 1931, and Rec.2020 on CIE color coordinates. f) Normalized PLQY and g) PL spectrum of CC-LED during aging in water. h) CCK-8 assay result of C2C12 mouse skeletal myoblast cells on OIHP NPs, CPN, and control film (sterilized-polystyrene cell culture plate) after 1, 3, 5 days. Data are presented as the mean ± standard deviation ($n = 4$). The inset shows photographs of CPN film in growth media (DMEM + FBS) (scale bar = 0.5 cm). i) Bright-field images of living cell cultured on CPN film. The cells were imaged after 1, 3, 5 days of culture. Scale bars in images are 50 µm.

passivates metallic Pb by electronic bonding, and thereby suppresses nonradiative recombination. Finally, we demonstrate green-emitting and white-emitting flexible large-area color-converting films based on CPN that are successfully operated under versatile bending and stable for >400 d in ambient air at RT and in water. Moreover, our CPN showed high stability

and excellent biocompatibility during cell proliferation in water. Our materials design strategy enables the use of perovskite NPs in highly stable luminescent materials of display devices and bio-related applications that require high stability under water and harsh environments.

Supporting Information

Supporting Information is available from the Wiley Online Library or from the author.

Conflict of Interest

The authors declare no conflict of interest.

Author Contributions

J.J., Y.-H.K., and S.P. contributed equally to this work. J.J., Young-Hoon Kim, and S.P. designed and conducted most experiments, analyzed all the data, synthesized OIHP NPs, and fabricated CPN. D.Y. and Yong-Hyun Kim performed first-principle DFT calculations and discussed results. H.C. helped in the synthesis of OIHP NPs. J.J. and C.B.P. helped and discussed biocompatibility test of the CPN. H.B.J. and J.M.Y. helped measurement and analysis of the TEM images. H.L. helped in the fabrication of CPN. D.Y. and Yong-Hyun Kim helped to revise the manuscript. D.Y.J. supervised S.P. and H.C. T.-W.L. and B.-S.B. initiated this work, designed experiments, and supervised every experiment in detail. The manuscript was mainly written by J.J., Young-Hoon Kim, S.P., B.-S.B., and T.-W.L.

[1] J. Luo, X. Wang, S. Li, J. Liu, Y. Guo, G. Niu, L. Yao, Y. Fu, L. Gao, Q. Dong, C. Zhao, M. Leng, F. Ma, W. Liang, L. Wang, S. Jin, J. Han, L. Zhang, J. Etheridge, J. Wang, Y. Yan, E. H. Sargent, J. Tang, *Nature* **2018**, *563*, 541.

[2] B. R. Sutherland, E. H. Sargent, *Nat. Photonics* **2016**, *10*, 295.

[3] A. Swarnkar, A. R. Marshall, E. M. Sanehira, B. D. Chernomordik, D. T. Moore, J. A. Christians, T. Chakrabarti, J. M. Luther, *Science* **2016**, *354*, 92.

[4] NREL Best Research-Cell Efficiencies, https://www.nrel.gov/pv/assets/pdfs/best-research-cell-efficiencies.20190802.pdf (accessed: September 2019).

[5] H. Cho, S.-H. Jeong, M.-H. Park, Y.-H. Kim, C. Wolf, C.-L. Lee, J. H. Heo, A. Sadhanala, N. Myoung, S. Yoo, T.-W. Lee, *Science* **2015**, *350*, 1222.

[6] a) Y.-H. Kim, H. Cho, T.-W. Lee, *Proc. Natl. Acad. Sci. USA* **2016**, *113*, 11694; b) H. Lee, J. Park, S. Kim, S.-C. Lee, Y.-H. Kim, T.-W. Lee, *Adv. Mater. Technol.* **2020**, 2000091.

[7] W. Xu, Q. Hu, S. Bai, C. Bao, Y. Miao, Z. Yuan, T. Borzda, A. J. Barker, E. Tyukalova, Z. Hu, M. Kawecki, H. Wang, Z. Yan, X. Liu, X. Shi, K. Uvdal, M. Fahlman, W. Zhang, M. Duchamp, J.-M. Liu, A. Petrozza, J. Wang, L.-M. Liu, W. Huang, F. Gao, *Nat. Photonics* **2019**, *13*, 418.

[8] T. Chiba, Y. Hayashi, H. Ebe, K. Hoshi, J. Sato, S. Sato, Y.-J. Pu, S. Ohisa, J. Kido, *Nat. Photonics* **2018**, *12*, 681.

[9] a) F. Zhang, H. Zhong, C. Chen, X.-g. Wu, X. Hu, H. Huang, J. Han, B. Zou, Y. Dong, *ACS Nano* **2015**, *9*, 4533; b) H. Zhou, J.-W. Park, Y. Lee, J.-M. Park, J.-H. Kim, J.-S. Kim, J.-H. Lee, S.-H. Jo, X. Cai, L. Li, X. Sheng, H.-J. Yun, J.-W. Park, J.-Y. Sun, T.-W. Lee, *Adv. Mater.* **2020**, *32*, 2001989.

[10] E. Jang, S. Jun, H. Jang, J. Lim, B. Kim, Y. Kim, *Adv. Mater.* **2010**, *22*, 3076.

[11] H. Y. Kim, D.-E. Yoon, J. Jang, D. Lee, G.-M. Choi, J. H. Chang, J. Y. Lee, D. C. Lee, B.-S. Bae, *J. Am. Chem. Soc.* **2016**, *138*, 16478.

[12] H. Kang, S. Kim, J. H. Oh, H. C. Yoon, J. H. Jo, H. Yang, Y. R. Do, *Adv. Opt. Mater.* **2018**, *6*, 1701239.

[13] S. J. Yang, J. H. Oh, S. Kim, H. Yang, Y. R. Do, *J. Mater. Chem. C* **2015**, *3*, 3582.

[14] A. Kakekhani, R. N. Katti, A. M. Rappe, *APL Mater.* **2019**, *7*, 041112.

[15] O. Hentz, Z. Zhao, S. Gradečak, *Nano Lett.* **2016**, *16*, 1485.

[16] G. Niu, X. Guo, L. Wang, *J. Mater. Chem. A* **2015**, *3*, 8970.

[17] a) Y.-H. Kim, C. Wolf, Y.-T. Kim, H. Cho, W. Kwon, S. Do, A. Sadhanala, C. G. Park, S.-W. Rhee, S. H. Im, T.-W. Lee, *ACS Nano* **2017**, *11*, 6586; b) J. Park, H. M. Jang, S. Kim, S. H. Jo, T.-W. Lee, *Trends Chem.* **2020**, *2*, 837.

[18] S. Kumar, J. Jagielski, T. Marcato, S. F. Solari, C.-J. Shih, *J. Phys. Chem. Lett.* **2019**, *10*, 7560.

[19] S. Huang, Z. Li, L. Kong, N. Zhu, A. Shan, L. Li, *J. Am. Chem. Soc.* **2016**, *138*, 5749.

[20] H. Hu, L. Wu, Y. Tan, Q. Zhong, M. Chen, Y. Qiu, D. Yang, B. Sun, Q. Zhang, Y. Yin, *J. Am. Chem. Soc.* **2018**, *140*, 406.

[21] A. Mehta, J. Im, B. H. Kim, H. Min, R. Nie, S. I. Seok, *ACS Nano* **2018**, *12*, 12129.

[22] Q. Zhou, Z. Bai, W. g. Lu, Y. Wang, B. Zou, H. Zhong, *Adv. Mater.* **2016**, *28*, 9163.

[23] H. Sun, Z. Yang, M. Wei, W. Sun, X. Li, S. Ye, Y. Zhao, H. Tan, E. L. Kynaston, T. B. Schon, H. Yan, Z.-h. Lu, G. A. Ozin, E. H. Sargent, D. S. Seferos, *Adv. Mater.* **2017**, *29*, 1701153.

[24] X. Zhang, H. Liu, W. Wang, J. Zhang, B. Xu, K. L. Karen, Y. Zheng, S. Liu, S. Chen, K. Wang, *Adv. Mater.* **2017**, *29*, 1606405.

[25] S. V. S. Rana, *J. Trace Elem. Med. Biol.* **2008**, *22*, 262.

[26] X. Gao, Y. Cui, R. M. Levenson, L. W. Chung, S. Nie, *Nat. Biotechnol.* **2004**, *22*, 969.

[27] L. Protesescu, S. Yakunin, M. I. Bodnarchuk, F. Krieg, R. Caputo, C. H. Hendon, R. X. Yang, A. Walsh, M. V. Kovalenko, *Nano Lett.* **2015**, *15*, 3692.

[28] X. Shang, X. Cao, Y. Ma, J. J. Kumaravel, K. Zheng, J. Zhang, R. Zhang, *Eur. Polym. J.* **2018**, *106*, 53.

[29] C. Peng, J. Chen, H. Wang, P. Hu, *J. Phys. Chem. C* **2018**, *122*, 27340.

[30] Z. Liu, Y. Bekenstein, X. Ye, S. C. Nguyen, J. Swabeck, D. Zhang, S.-T. Lee, P. Yang, W. Ma, A. P. Alivisatos, *J. Am. Chem. Soc.* **2017**, *139*, 5309.

[31] D. Shi, V. Adinolfi, R. Comin, M. Yuan, E. Alarousu, A. Buin, Y. Chen, S. Hoogland, A. Rothenberger, K. Katsiev, Y. Losovyj, X. Zhang, P. A. Dowben, O. F. Mohammed, E. H. Sargent, O. M. Bark, *Science* **2015**, *347*, 519.

[32] T.-H. Han, J.-W. Lee, C. Choi, S. Tan, C. Lee, Y. Zhao, Z. Dai, N. De Marco, S.-J. Lee, S.-H. Bae, Y. Yuan, H. M. Lee, Y. Huang, Y. Yang, *Nat. Commun.* **2019**, *10*, 520.

[33] Y. Wang, J. He, H. Chen, J. Chen, R. Zhu, P. Ma, A. Towers, Y. Lin, A. J. Gesquiere, S.-T. Wu, Y. Dong, *Adv. Mater.* **2016**, *28*, 10710.

[34] R. Brenes, D. Guo, A. Osherov, N. K. Noel, C. Eames, E. M. Hutter, S. K. Pathak, F. Niroui, R. H. Friend, M. S. Islam, H. J. Snaith, V. Bulovic, T. J. Savenije, S. D. Stranks, *Joule* **2017**, *1*, 155.

[35] X. Huang, T. R. Paudel, P. A. Dowben, S. Dong, E. Y. Tsymbal, *Phys. Rev. B* **2016**, *94*, 195309.